1521-0103/12/3412-543–551$25.00
THE JOURNAL OF PHARMACOLOGY AND EXPERIMENTAL THERAPEUTICS
Vol. 341, No. 2
190942/3766519
JPET 341:543–551, 2012

Charge and Geometry of Residues in the Loop 2 β Hairpin Differentially Affect Agonist and Ethanol Sensitivity in Glycine Receptors

Daya I. Perkins,[1] James R. Trudell, Liana Asatryan, Daryl L. Davies, and Ronald L. Alkana

Alcohol and Brain Research Laboratories, Departments of Pharmacology and Pharmaceutical Sciences (D.I.P., R.L.A.) and Clinical Pharmacy and Pharmaceutical Economics and Policy (L.A., D.L.D.), School of Pharmacy, University of Southern California, Los Angeles, California; and Department of Anesthesia and Beckman Program for Molecular and Genetic Medicine, Stanford School of Medicine, Stanford, California (J.R.T.)

Received December 9, 2011; accepted February 21, 2012

ABSTRACT

Recent studies highlighted the importance of loop 2 of α1 glycine receptors (GlyRs) in the propagation of ligand-binding energy to the channel gate. Mutations that changed polarity at position 52 in the β hairpin of loop 2 significantly affected sensitivity to ethanol. The present study extends the investigation to charged residues. We found that substituting alanine with the negative glutamate at position 52 (A52E) significantly left-shifted the glycine concentration response curve and increased sensitivity to ethanol, whereas the negative aspartate substitution (A52D) significantly right-shifted the glycine EC_{50} but did not affect ethanol sensitivity. It is noteworthy that the uncharged glutamine at position 52 (A52Q) caused only a small right shift of the glycine EC_{50} while increasing ethanol sensitivity as much as A52E. In contrast, the shorter uncharged asparagine (A52N) caused the greatest right shift of glycine EC_{50} and reduced ethanol sensitivity to half of wild type. Collectively, these findings suggest that charge interactions determined by the specific geometry of the amino acid at position 52 (e.g., the 1-Å chain length difference between aspartate and glutamate) play differential roles in receptor sensitivity to agonist and ethanol. We interpret these results in terms of a new homology model of GlyR based on a prokaryotic ion channel and propose that these mutations form salt bridges to residues across the β hairpin (A52E-R59 and A52N-D57). We hypothesize that these electrostatic interactions distort loop 2, thereby changing agonist activation and ethanol modulation. This knowledge will help to define the key physical-chemical parameters that cause the actions of ethanol in GlyRs.

Introduction

Studies over the last decade point to a role for glycine receptors (GlyRs) in mediating at least a subset of the behavioral effects of ethanol. Those studies found that behaviorally relevant concentrations of ethanol positively modulate GlyR function measured in a variety of preparations (for review, see Perkins et al., 2010). Other studies suggest that GlyRs in the nucleus accumbens are targets for ethanol that are involved in ethanol-induced mesolimbic dopamine release (Molander and Söderpalm, 2005; Molander et al., 2007), thus linking GlyRs to the rewarding effects of ethanol.

Experiments using molecular strategies combined with a novel ethanol antagonist, increased atmospheric pressure, pointed to extracellular domain loop 2 of GlyRs as an important target for ethanol action (Davies et al., 2004; Perkins et al., 2008, 2010). Other studies, using the substituted cysteine accessibility method (Karlin and Akabas, 1998) with the alcohol-like reagent propyl methanethiosulfonate (MTS), identified position 52 (Ala52) in loop 2 of the extracellular domain (Crawford et al., 2007) and position 267 (Ser267) in the transmembrane (TM) domain (Mihic et al., 1997) as sites of ethanol action in GlyRs. Further investigation suggested that position 52 in the extracellular domain and position 267 in the TM domain form part of a contiguous alcohol-action pocket (Crawford et al., 2007).

Subsequent studies found a relationship between polarity, but not molecular volume, of the residue at position 52 and

This work was supported in part by the National Institutes of Health National Institute on Alcohol Abuse and Alcoholism [Grants F31-AA017569 (to D.I.P.), RO-1-AA03972 (to R.L.A.), RO-1-AA013922 (to D.L.D.), RO-1-AA013378 to J.R.T.]; the Southern California Translational Research Institute [Pilot Award 1UL1RR031986-01] (to R.L.A.); and the University of Southern California School of Pharmacy.

This work was conducted as partial fulfillment of the requirements for the Ph.D degree in Molecular Pharmacology and Toxicology at the University of Southern California for D.I.P.

[1]Current affiliation: Allergan, Inc., Irvine, California.

Article, publication date, and citation information can be found at http://jpet.aspetjournals.org.

http://dx.doi.org/10.1124/jpet.111.190942.

ABBREVIATIONS: GlyR, glycine receptor; GLIC, *Gloeobacter violaceus* pentameric ligand-gated ion channel homolog; MTS, methanethiosulfonate; MTSES, MTS sodium salt; WT, wild type; TM, transmembrane; $GABA_AR$, γ-aminobutyric acid type A receptor.

ethanol sensitivity in α1GlyRs (Perkins et al., 2008). Neither polarity nor molecular volume at position 52 consistently altered agonist sensitivity in GlyRs (Perkins et al., 2008).

Those earlier studies on polarity investigated only ethanol sensitivity when uncharged, but polar, residues were substituted at position 52. This leaves open the question of whether this relationship extends to the much higher degree of polarity that would be produced by the substitution of charged residues.

Other studies further implicate the structure of loop 2 as a key determinant of ethanol sensitivity in GlyRs and γ-aminobutyric acid type A receptors ($GABA_A$Rs) (Perkins et al., 2009). Those investigations took advantage of prior work indicating that δ-subunit-containing $GABA_A$Rs (e.g., α4β3δ), in contrast to other $GABA_A$Rs (e.g., α1β2γ2), are sensitive to ethanol concentrations as low as 3 mM (Wallner et al., 2003; Mody et al., 2007; Olsen et al., 2007; Santhakumar et al., 2007; Meera et al., 2010). Those studies tested whether the structure of loop 2 in $GABA_A$R δ could play a role in this increased ethanol sensitivity. This was accomplished by mutating the nonconserved residues of loop 2 in α1 GlyRs to the corresponding residues found in $GABA_A$R δ loop 2 (Perkins et al., 2009). This loop 2 substitution in WT α1GlyRs reduced the threshold for ethanol sensitivity from 30 mM in WT GlyRs to 1 mM in the δ loop 2 mutant and increased the degree of ethanol potentiation. Moreover, mutating loop 2 of the γ subunit of α1β2γ2 $GABA_A$Rs to the homologous sequence in the $GABA_A$R δ subunit shifted the threshold for ethanol sensitivity from 50 mM in WT to 1 mM in the corresponding chimera and, as in GlyR, markedly increased the magnitude of the ethanol response versus WT $GABA_A$Rs.

Our interest in the role of loop 2 in GlyR function was increased by investigations that showed a key role for loop 2 in the gating process (Cederholm et al., 2010). Cederholm et al. prepared cysteine mutations of each residue in loop 2 and then measured the rate of activation of these mutants by MTS reagents. From the rate measurements, they were able to infer differential accessibility between the resting and activated states, thereby highlighting residues associated with signal transduction. In addition, Pless and Lynch (2009) covalently attached a fluorescent analog to A52C and were able to infer conformational changes in GlyR loop 2 that correlated with agonist efficacy.

The present study tested the hypothesis that the degree of polarity at position 52 can significantly affect the sensitivity of the receptor to ethanol. This hypothesis predicts that substituting highly charged polar residues at position 52 would modulate ethanol sensitivity more than substituting polar but uncharged residues. Unexpectedly, we found that it was essential to consider both charge and the specific geometries of individual residues to understand the effects of the mutations on agonist and ethanol sensitivity. This requirement led us to develop a new model of the GlyR, which depicts the mutations as salt bridges spanning the β hairpin in loop 2 and provides insight into the structures and mechanisms of glycine and ethanol action.

Materials and Methods

Materials. Adult female *Xenopus laevis* frogs were purchased from Nasco (Fort Atkinson, WI). Penicillin, streptomycin, gentamicin, 3-aminobenzoic acid ethyl ester, glycine, ethanol, and collagenase were purchased from Sigma (St. Louis, MO). All other chemicals used were of reagent grade.

Expression in Oocytes. *X. laevis* oocytes were isolated and injected with WT, human α1, or mutant α1A52C, α1A52D, α1A52E, α1A52H, α1A52K, α1A52N, α1A52Q or α1A52R cDNAs (1 ng per 32 nl) cloned into the mammalian expression vector pCIS2 or pBKCMV as described previously (Davies et al., 2003) and verified by partial sequencing (DNA Core Facility, University of Southern California, Los Angeles, CA). Mutagenesis of the alanine at position 52 in α1GlyRs was performed as described previously (Davies et al., 2003). After injection, oocytes were stored individually in incubation medium (modified Barth's solution supplemented with 2 mM sodium pyruvate, 0.5 mM theophylline, 10,000 U/l penicillin, 10 mg/l streptomycin, and 50 mg/l gentamicin) in Petri dishes (VWR, San Dimas, CA). All solutions were sterilized by passage through 0.22-μM filters. Oocytes, stored at 18°C, usually expressed GlyRs the day after injection. Oocytes were used in α recordings for 3 to 7 days after cDNA injection. Note that heteromeric α1β GlyRs predominate over homomeric α1 GlyRs in adult human brain and these heteromeric receptors can differ from homomeric receptors in ethanol sensitivity (Rajendra et al., 1997). However, prior work in recombinant systems found no differences between homomeric α1 GlyRs and heteromeric α1β GlyRs in responsiveness to glycine (Lynch, 2004). More important, homomeric α1 GlyRs have been the primary focus of molecular modeling studies (Webb and Lynch, 2007; Perkins et al., 2010). Therefore, we used homomeric α-1 GlyRs in the present study.

Two-Electrode, Whole-Cell, Voltage-Clamp Recordings. Two-electrode, voltage-clamp recordings were performed by using techniques similar to those reported previously (Davies et al., 2003). All electrophysiological recordings were conducted within an oocyte bath, two micro positioners (WPI, Sarasota, FL or Narishige, Greenvale, NY), and a bath clamp (Davies et al., 2003). Oocytes were perfused in a 100-μl oocyte bath at room temperature (20–23°C) with modified Barth's solution ± drugs at 2 ml/min using 1/16 o.d. high-pressure PEEK tubing (Upchurch Scientific, Oak Harbor, WA). Oocytes were voltage-clamped at a membrane potential of −70 mV by using a Warner Instruments (Hamden, CT) oocyte clamp (model OC-725C).

Glycine Concentration Responses. Oocytes expressing WT or mutant α1GlyRs were exposed to glycine for 30 s, using 5- to 15-min washouts between applications to ensure complete resensitization (Mascia et al., 1996a,b; Davies et al., 2004; Crawford et al., 2007). Pilot experiments found that WT and mutant GlyR agonist responses, using a 1-min glycine application, reached a steady-state equilibrium with results that did not differ appreciably from results using 30-s applications. Therefore, we used the shorter application time to increase efficiency and minimize desensitization at the higher glycine concentrations. Responses were normalized to the maximal glycine response. Concentration response curves were analyzed by using nonlinear regression.

Ethanol Experiments. Previous work found that ethanol potentiation of GlyR function is more robust and reliable when tested in the presence of low concentrations of glycine (typically EC_{2-10}) (Davies et al., 2004; Perkins et al., 2008). This is because the largest effects of potentiation are seen at low agonist concentrations and are essentially masked at I_{max}. Based on these studies, we used a concentration of glycine producing 2 ± 0.3% of the maximal effect (EC_2). When testing ethanol potentiation, the oocytes were preincubated with ethanol for 60 s before coapplication of ethanol and glycine (Davies et al., 2004). Washout periods (5–15 min) were allowed between drug applications to ensure complete resensitization of receptors. Note that ethanol is a low-efficacy drug in that millimolar concentrations are associated with behavioral signs of intoxication (17 mM for driving under the influence in California). In studies of ethanol action on ion channels, concentrations of ethanol (10–100 mM) typically produce responses in the 15 to 40% range. Therefore, we used 100 mM ethanol in the present studies to reduce variability inherent with such small changes. All experiments testing mutant

GlyRs included WT control receptors expressed in the same batch of oocytes as the respective mutant GlyRs.

MTS Reagent Protocol. We used charged MTS reagents in combination with cysteine substitutions as an alternative approach to introducing charged mutations for assessing the effect of charge at position 52 on sensitivity to glycine and ethanol. Previous work found that positions 52 and 53 are accessible to and capable of binding MTS reagents (Crawford et al., 2007, 2008; Cederholm et al., 2010). Oocytes expressing WT or A52C GlyRs were exposed to negatively charged 2-sulfonatoethyl MTS sodium salt (MTSES) (10 mM) for 2 min to saturate the substituted cysteine residues with covalent disulfide bonds to the reagent. After the saturation exposure, oocytes were transferred to the recording chamber and tested as described above for the glycine concentration-response study. MTS solutions were prepared immediately before testing. Prior work has shown that saturating the oocyte with MTSES in this manner yielded results that did not differ appreciably from results obtained by perfusing MTSES (Crawford et al., 2008).

Cell-Surface Biotinylation and Immunoblotting. Biotinylation of surface-expressed proteins was performed as described previously (Chen et al., 2005; Perkins et al., 2009). Surface proteins of oocytes (15 oocytes per group) expressing GlyRs were incubated with 1.5 mg/ml membrane-impermeable Sulfo-NHS-SS-biotin (Thermo Fisher Scientific, Waltham, MA) and after washes homogenized in lysis buffer [40 mM Tris, pH 7.5, 110 mM NaCl, 4 mM EDTA, 0.08% Triton X-100, and 1% protease inhibitor cocktail (Vector Laboratories, Burlingame, CA)]. The yolk and cellular debris were removed by centrifugation at 3600*g* for 10 min, and aliquots of the supernatants were stored at −20°C to assess total receptor fraction. The remaining supernatant was incubated with streptavidin beads (Thermo Fisher Scientific) overnight at 4°C, and the biotinylated proteins were eluted using SDS loading buffer. The surface and total proteins were separated using SDS-polyacrylamide gel electrophoresis and transferred to polyvinylidene difluoride membranes, and the immunoblotting was performed by using rabbit anti-GlyR antibody (1:500 dilution; Millipore Bioscience Research Reagents, Temecula, CA) and horseradish peroxidase-conjugated secondary antibody. Protein bands were visualized using enhanced chemiluminescence (Pierce Biotechnology). The blots were then scanned and analyzed using Scion Image software (Scion Corporation, Frederick, MD).

Molecular Modeling. Our ability to interpret the previous and present results in terms of a homology model was greatly aided by publications about the X-ray structure of *Gloeobacter violaceus* pentameric ligand-gated ion channel homolog (GLIC), a prokaryotic proton-gated channel with high structural homology to GlyRs (Bocquet et al., 2009). Loop 2 in GLIC is essentially identical to the corresponding loop 2 in the X-ray structure of the glutamate chloride channel (Hibbs and Gouaux, 2011). We chose to prepare a homology model based on GLIC because long time-scale molecular dynamics studies in GLIC (Nury et al., 2010, 2011; Zhu and Hummer, 2010) have allowed us to interpret interactions of salt bridges between the ligand-binding extracellular and TM domains of GlyR (Kash et al., 2003) in terms of dynamic interactions on the microsecond time scale (Murail et al., 2011).

In the present study, we built a new homology model of GlyR by threading the primary sequence of GlyR onto the X-ray structure of GLIC (Bocquet et al., 2009). The alignment of GlyR with GLIC was as described by Perkins et al. (2009).

An important point in the present model is that GlyR has four more residues than GLIC in the region of Ala82 in 3EAM. We tried several models in which these four residues were distributed into the aligned structure; we found that grouping all four residues together into the loop after Ala82 in 3EAM produced the best structure without serious van der Waals overlaps. The resulting alignment (Bertaccini et al., 2010) is essentially identical to that described by Cederholm et al. (2010) (Baenziger and Corringer, 2011).

The homology model of GlyR was built with the Modeler module of Discovery Studio 2.5.5 (Accelrys, San Diego, CA) with the alignment described above and the additional restriction that the Cys-loop disulfide bond in all five subunits of GlyR (Cys138–Cys152) should be preserved. We built 50 models and selected the "best" based on total force field energy. The Side Chain Refinement module of Discovery Studio was used to optimize possible rotamers and side-chain packing. Then we applied a harmonic restraint of 10 kcal/(mol × Å^2) restraint on all backbone atoms and optimized the model to an energy gradient of 0.0001 kcal/Å by using the CHARMm force field and the default spherical nonbond cutoff of 14 Å. The model was relaxed with 50,000 1-fs steps of molecular dynamics at 300 K. We than selected the two most significant mutations in this study (Table 1) [A52E (glycine EC_{50} of 31 μM compared with WT 374 μM; Table 1) and A52N (glycine EC_{50} of 13,358 μM)] and built models with these mutations, based on the WT model described above. In each of the "mutant" models, we manually selected rotamers of A52E or A52N that could interact with other residues in loop 2 by using the Ponder and Richards criteria in the Side Chain Refinement module of Discovery Studio 2.5 (Ponder and Richards, 1987). We found two especially favorable pairs of residues that formed salt bridges across loop 2 in these models: A52E with Arg59 and A52N with Asp57.

We sought to observe the possible interactions of these pairs of residues and the effect of these mutations on the structure of loop 2. Three models were used: the WT model described above and the two mutations in which rotamers of the A52E and A52N mutations had been adjusted manually to form salt bridges. To focus on these interactions within loop 2, we fixed the positions of all backbone atoms in the three models, except those in loop 2 positions 50 and 60, and then ran molecular dynamics simulations of 1,000,000 1-fs steps at 300K with the CHARMm force field and the default setting for CHARMm described above.

The large difference in responses observed between the A52D and A52E mutations suggested that relatively small geometric changes were critical. We built the default conformations of single aspartate and glutamate residues and manually superimposed them with a slight offset to display both residues. Then we measured the C-α to C (O_2) carbons.

TABLE 1

Summary of nonlinear regression analysis results for glycine concentration responses of WT and mutant α1 GlyRs

Glycine EC_{50}, Hill slope (n_H), and maximal current amplitude (I_{max}) are presented as mean ± S.E.M. from four to seven different oocytes shown in Fig. 1. There was no significant difference between WT and mutant GlyRs in maximal current amplitude (I_{max}) with the exception of α1A52N.

Charge at Position 52	Receptor	I_{max}	Hill Slope	EC_{50}
		nA		*μM*
Negative	α1A52E	10595 ± 1516	4.513 ± 0.725	31.28 ± 2.9*
	α1A52D	8813 ± 188	3.312 ± 0.694	587.08 ± 80*
Neutral	α1WT	7650 ± 602	3.094 ± 0.879	374.17 ± 24
	α1A52N	1605 ± 339*	1.210 ± 0.204*	13358.71 ± 2294.34**
	α1A52Q	11962 ± 5018	1.774 ± 0.515	407.50 ± 213.24
Positive	α1A52R	10095 ± 2587	1.876 ± 0.170	313.10 ± 94.7
	α1A52H	15770 ± 5640	2.397 ± 0.260	385.33 ± 130.7
	α1A52K	8068 ± 1134	2.326 ± 0.467	148.16 ± 33.21

*, $P < 0.05$; **, $P < 0.01$ vs. WT α1GlyRs.

Data Analysis. Data for each experiment were obtained from oocytes from at least two different frogs. Results are expressed as mean ± S.E.M. Where no error bars are shown in the figures, they are smaller than the symbols. We used Prism (GraphPad Software Inc., San Diego, CA) to perform curve fitting and statistical analyses. Concentration response data were analyzed by using nonlinear regression analysis: $[I = I_{max}\ [A]^{nH}/([A]^{nH} + EC_{50}{}^{nH})]$, where I is the peak current recorded after application of a range of agonist concentrations, [A]; I_{max} is the estimated maximum current; EC_{50} is the glycine concentration required for a half-maximal response and n_H is the Hill slope. Data were subjected to t tests and one- or two-way analysis of variance with Dunnett's multiple comparison tests when warranted. Statistical significance was defined as $p < 0.05$.

Results

Position 52 and Agonist Sensitivity

Charge and Structure of Amino Acids at Position 52 Are Important for Agonist Sensitivity in α1GlyRs. We found a significant left shift in glycine EC_{50} from WT α1GlyR for the negatively charged α1A52E and a significant right shift for the negatively charged α1A52D (Fig. 1; Table 1). Substituting glutamine, the uncharged structural analog of glutamate at position 52 (α1A52Q) did not cause a similar left shift in glycine response. Substituting asparagine, the uncharged structural analog of aspartate at position 52 (α1A52N) caused a significant increase in EC_{50} and a significant right shift in glycine concentration response larger than that observed for α1A52D (Fig. 1; Table 1). Positively charged residues at position 52 did not cause significant shifts in EC_{50}. With the exception of the A52N mutant, no significant differences were observed between WT and mutant GlyRs in Hill slope (n_H) or maximal current amplitude (I_{max}) (Table 1). Collectively, these changes in glycine sensitivity were consistent with the notion that a negative charge at position 52 affects agonist sensitivity in GlyRs. However, the effects of substituting glutamate and aspartate were in opposite directions and seemed to reflect differences in side-chain geometries. These results suggest that specific interactions (possibly salt bridges), which depend on geometric differences that are as small as 1 Å, as seen in the aspartate-to-glutamate mutation, are responsible for the significant shifts in I_{max} and Hill slope.

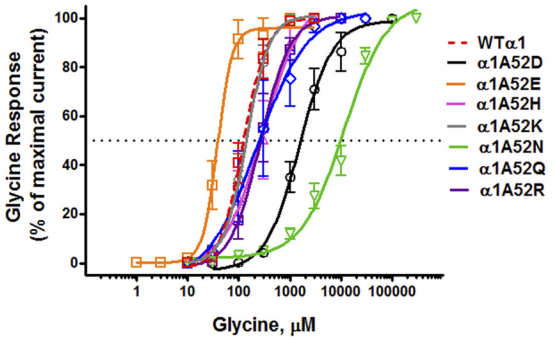

Fig. 1. Concentration-response curves for glycine-activated chloride currents in *X. laevis* oocytes expressing WT and mutant α1GlyR subunits. Glycine-induced chloride currents were normalized to the maximal current activated by a saturating concentration of glycine (30 mM). The curves represent nonlinear regression analysis of the glycine concentration responses in the α1 mutant GlyRs compared with WT α1GlyRs. Details of EC_{50}, Hill slope, and maximal current amplitude (I_{max}) are provided in Table 1. Glycine was applied for 30 s. Washout time was 5 to 15 min after the application of glycine. Each data point represents the mean ± S.E.M. from eight different oocytes.

Cell Surface Expression of WT and Mutant α1GlyRs. To determine whether the shifts in I_{max} responses of A52N GlyRs reflected changes in surface expression levels, we compared the GlyR protein content of WT and mutant GlyRs via cell-surface biotinylation and immunoblotting analysis (Fig. 2). We did not observe any notable differences between cell surface or total expression of GlyR protein between WT and any of the mutant GlyRs tested. This finding, in conjunction with the change in the response of A52N to glycine, compared with WT GlyRs, is consistent with the interpretation that the mutation causes a change in the functional response of the receptor.

Binding a Negatively Charged MTS Reagent at Position 52 Is Not Sufficient to Affect Glycine Sensitivity. To test independently the role of a negative charge at position 52 on agonist sensitivity, we substituted a cysteine at position 52 and then covalently bound a negatively charged MTSES reagent to the substituted cysteine residue. Replacing the neutral alanine at position 52 in WT GlyRs with the neutral cysteine (A52C) right-shifted the glycine concentration response (Fig. 3). Exposure to negatively charged MTSES did not significantly affect the response of the A52C mutant to glycine (Fig. 3). These results suggest that negative charge alone is insufficient to alter agonist sensitivity in GlyRs. Rather, the presence of a negative charge in combination with the appropriate structure is necessary. This result is consistent with the large differences we observed between the A52D and A52E mutations (Fig. 1).

Position 52 and Ethanol Sensitivity

The Structure of the Amino Acid at Position 52 Affects Ethanol Sensitivity. The effect of charged substitutions at position 52 in α1GlyRs on sensitivity to 100 mM ethanol is shown in Fig. 4A. Ethanol responses for the negatively charged α1A52E were significantly increased compared with WT α1GlyRs. In contrast, the negatively charged A52D mutation did not differ from WT with respect to ethanol sensitivity. Ethanol responses for the positively charged substitutions at position 52 (α1A52H, α1A52K, and α1A52R) were not significantly different from WT α1GlyRs (Fig. 4A). Overall, these findings did not correspond to the effects these substitutions had on agonist sensitivity and suggest that a combination of charge and specific salt-bridge interactions at position 52 in α1GlyRs are required to affect ethanol sensitivity.

To investigate further a possible role for the structure of the amino acid at position 52 in modulating ethanol sensitiv-

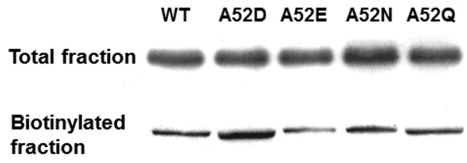

Fig. 2. Cell surface expression of WT and mutant α1GlyRs. Western blot analysis of total cell lysate and cell-surface biotinylated fraction from *X. laevis* oocyte expression of WT, A52D, A52E, A52N, or A52Q GlyRs. Results shown are for 1 ng of WT or mutant GlyR cDNA injected into each oocyte. Protein lysates were run on SDS-polyacrylamide gel electrophoresis gel and then transferred to polyvinylidene difluoride membrane. Blots were then probed with rabbit antibody against the α1 subunit of the human GlyR.

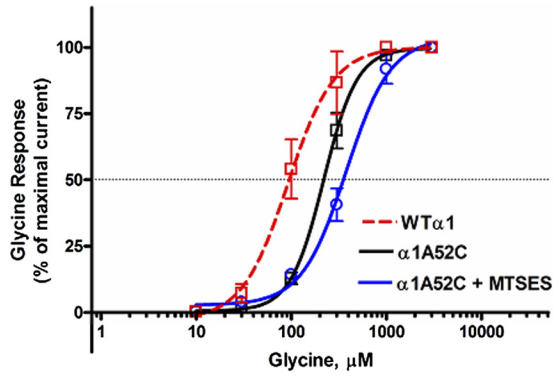

Fig. 3. Concentration-response curves for glycine-activated chloride currents in *X. laevis* oocytes expressing WT and A52C mutant α1GlyR subunits exposed to MTSES. Mutant A52C GlyRs were exposed to the negatively charged MTSES. The curves represent nonlinear regression analysis of the glycine concentration responses from four different oocytes expressing WT (red), A52C (black), or A52C (blue) GlyRs. The introduction of negative charge at position 52 did not significantly affect agonist sensitivity. Each data point represents the mean ± S.E.M.

ity, we substituted the uncharged structural analog of glutamate (glutamine) at position 52 (α1A52Q). This substitution resulted in a similar increase in ethanol sensitivity to that observed for A52E (Fig. 4B). It is noteworthy that substituting the uncharged structural analog of aspartate (asparagine) at position 52 (α1A52N) caused a significant decrease in ethanol sensitivity (Fig. 4B). These findings collectively indicate that subtle differences in the structure of the amino acid at position 52, rather than just charge, can have a major impact on ethanol sensitivity in α1GlyRs.

To test independently the role of substituting a negative charge at position 52 on ethanol sensitivity, we used the modified substituted cysteine accessibility method described above. Replacing the neutral alanine at position 52 in WT GlyRs with the neutral cysteine (A52C) significantly reduced ethanol response at 100 mM (Fig. 5). Exposure to negatively charged MTSES did not significantly affect the response of the A52C mutant to ethanol (Fig. 5). These results further support the contention that charge alone is insufficient to alter ethanol sensitivity in GlyRs.

Molecular Model. Molecular models based on the present findings support the conclusion that a combination of structure, polarity, and charge at position 52 affects both agonist and ethanol sensitivity, possibly by introducing salt bridges or H bonds across the β hairpin of loop 2 (Fig. 6). The findings with α1A52Q and α1A52N indicate that subtle differences in the chemical structure of the amino acid at position 52 can have a major impact on agonist and ethanol sensitivity in α1GlyRs.

An important point about the GlyR homology model based on GLIC (Fig. 6) is that Lys276 extends across the intersubunit space to form a triple salt bridge with Glu53 and Arg218 (Crawford et al., 2008; Bocquet et al., 2009; Perkins et al., 2009). This triple salt bridge was preserved, but distorted, during the molecular dynamics simulations of the three models of loop 2 described under *Materials and Methods* (Fig. 6, C–E). Although we initially thought that A52E or A52N might compete with this salt bridge, we found that the 180° orientation of the side chain of Ala52 versus Glu53 in a β strand was preserved, a result that agrees with recent cysteine substitutions in loop 2 by Cederholm et al. (2010). We

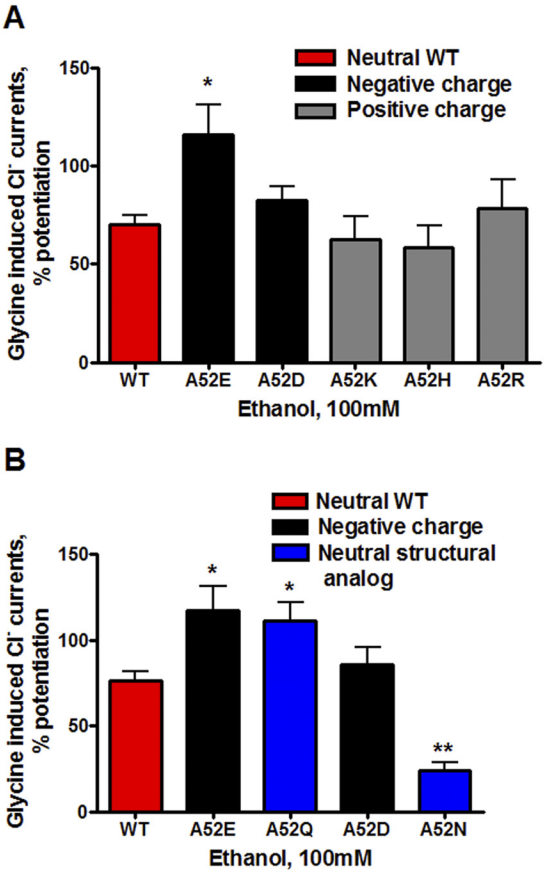

Fig. 4. The effects of charge (A) and structure (B) of the residue at position 52 in α1GlyRs on ethanol sensitivity. The percentage of potentiation of glycine-induced currents is shown for WT and mutant α1GlyRs. A, the red bar shows the WT GlyR, which has a neutral amino acid at position 52. Black bars represent negatively charged substitutions at position 52 in α1GlyRs, and gray bars represent positively charged substitutions. Charge does not have a consistent effect on ethanol sensitivity of α1GlyRs. B, the red bar shows the WT GlyR, which has a neutral amino acid at position 52. Black bars represent negatively charged A52E and A52D substitutions at position 52 in α1GlyRs. The blue bars represent the uncharged structurally analogous substitutions for Glu and Asp, A52Q and A52N, respectively. The structure of the amino acid at position 52 plays a role in ethanol sensitivity of α1GlyRs. Note that studies shown in A and B were run together. The WT and mutant A52E and A52D findings presented in B are the same as shown in A and are presented to facilitate comparison. *, $p < 0.05$ or **, $p < 0.01$ versus WT α1GlyRs for six to eight oocytes per group.

suggest that these mutations at Ala52 predominantly affect interactions within loop 2 (Fig. 6), not the triple salt bridge at the interface of the ligand binding and transmembrane domains (Kash et al., 2003; Nury et al., 2010, 2011). In particular, the A52E with Arg59 and A52N with Asp57 salt bridges were stable during the simulations, and their interactions produced significant changes in the structure of loop 2 during the steps of the simulations (Fig. 6, C–E).

It is interesting to observe the changes in loop 2 during the three molecular dynamics simulations. In the case of the WT loop 2, the overall structure of loop 2 remained stable during the simulation (Fig. 6C); the triple salt bridge between Glu53, Lys276, and Arg218 remained stable, and there was no interaction of Ala52 with either Asn57 or Arg59. In the case of the A52E mutation, we initially sought salt-bridge interactions with 52Glu by adjusting rotamer positions of neighboring residues. We found a strong salt bridge interac-

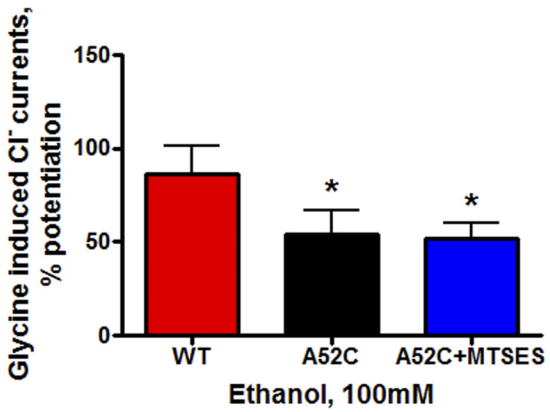

Fig. 5. The effects of ethanol on WT and A52C mutant α1GlyRs exposed to MTSES. Mutant A52C GlyRs were exposed to the negatively charged MTSES. The red bar shows mean ± S.E.M. for WT, the black bar indicates A52C, and the blue bar indicates the A52C exposed to MTSES. The introduction of negative charge at position 52 using MTSES did not significantly affect ethanol sensitivity. *, $p < 0.05$ versus WT α1GlyRs for four oocytes per group.

tion with A52E to Arg59 (Fig. 6D). After the simulation, this interaction pulled Arg59 over the top of Asn57 and distorted loop 2 as well as the triple salt bridge, including a change of the E53 salt bridge from a straight-on orientation to Arg218 to a side-on salt bridge. The mutation with the opposite change in glycine EC_{50}, A52N, produced a strong salt bridge with Asp57 (Fig. 6E). After the molecular dynamics simulation of this mutation, the salt bridge between A52N with Asp57 pulled Asp57 toward A52N and repelled Arg59. The triple salt bridge remained intact, but the plane of the carbonyl oxygen atoms of Glu53 had rotated and the interactions of Glu53 with Arg218 and Lys276 were altered. The extended dimensions of aspartate and glutamate differ by only 1 Å (Fig. 7), yet the large effects caused by their substitution suggests the network of interactions across the domain interface is critical for signal transmission.

Discussion

Prior studies found that the polarity of the residue at position 52 in α1GlyRs is highly correlated with the sensitivity of the receptor to ethanol (Perkins et al., 2008). The present study determined whether this relationship extended to charged amino acids. The findings support the hypothesis that charge interactions determined by the specific geometry of the amino acid at position 52 play differential roles in receptor sensitivity to agonist and ethanol. These new results highlight the importance of loop 2 in ethanol action. These differences in the role of charge and structure on sensitivity to ethanol seem to be independent of the changes caused by the mutations on agonist sensitivity and

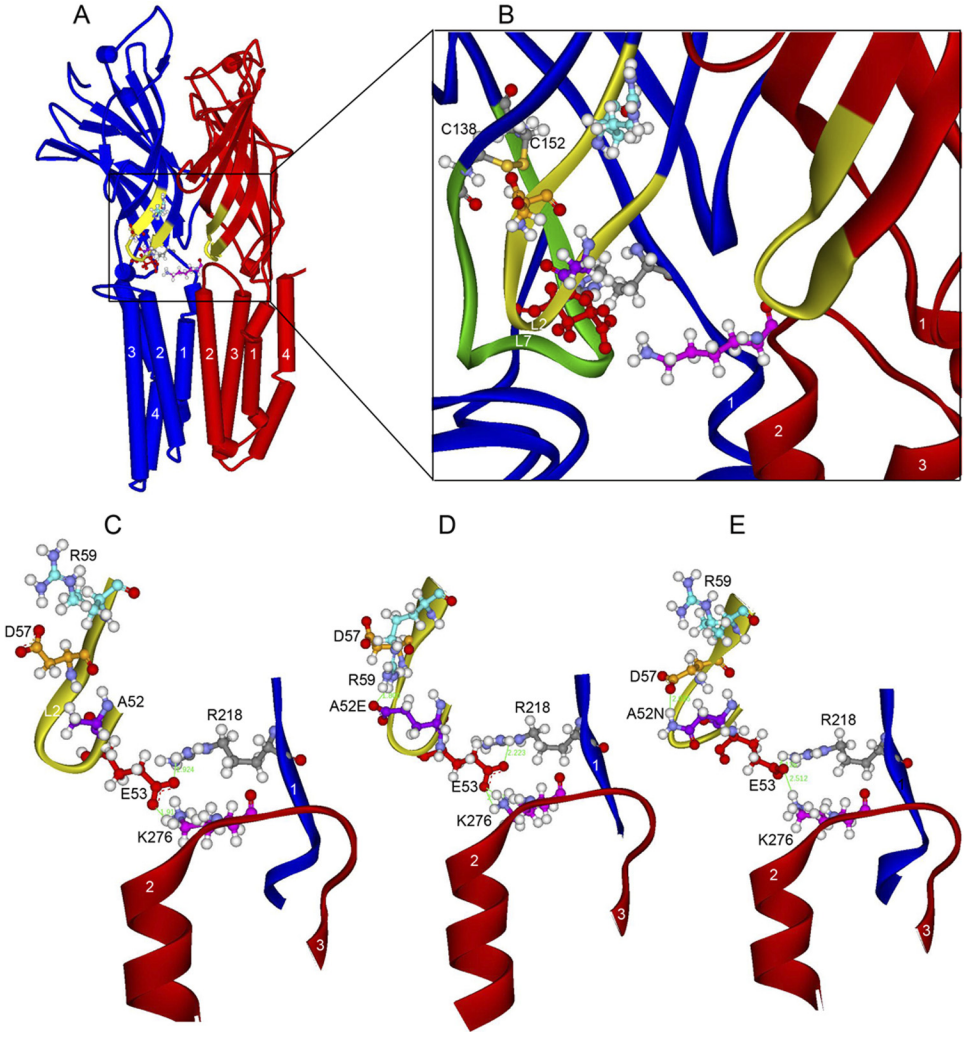

Fig. 6. Homology models of WT and mutant α1GlyRs based on GLIC. A, WT α1GlyR, a view of two subunits looking along the plane of the membrane from the center of the ion pore. We show two subunits because Lys276 bridges the gap between adjacent subunits (subunit containing Lys276 is colored red) and interacts with the subunit containing Glu53 (colored blue) of the adjacent subunit. B, domain interface in WT α1GlyR. Enlargement of the view in A showing a ribbon rendering of the backbone atoms of loop 2 (yellow portion of both subunits rendered in red and blue ribbons). The residues in the triple salt bridge of Glu53 (red), Arg218 (gray), and Lys276 (pink) are rendered in ball and stick. For reference, loop 7 (Cys-loop) is rendered in green ribbon, and the Cys-loop residues Cys138 and Cys152 are shown (sulfur atoms are orange). C, loop 2 in WT α1GlyR. Further enlargement of WT α1GlyR shown in B is focused on loop 2. The triple salt bridge is established but there are no interactions across the β hairpin of loop2. D, mutant A52E α1GlyR. View of loop 2 in A52E showing the new salt bridge of A52E with R59 and the resulting distortion of the backbone atoms of loop 2. E, mutant A52N α1GlyR. View of loop 2 in A52N showing the new salt bridge of A52N with Asp57 and the resulting distortion of the backbone atoms of loop 2. In the short molecular dynamics simulation, these changes in loop 2 produced small changes in the triple salt bridge of Glu53, Arg218, and Lys276.

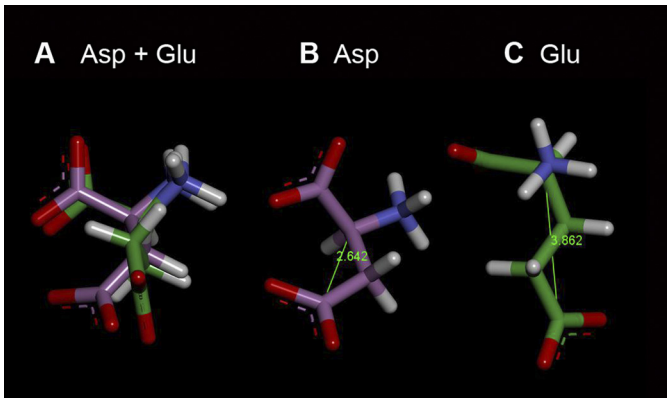

Fig. 7. Substituting different amino acids at position 52 alters the geometry of α1GlyRs. A, aspartate (Asp) and glutamate (Glu). The models of the Asp and Glu residues were superimposed and then slightly offset to reveal the distinct colors of the backbone carbons and show the increased length of the Glu side chain. All distances and dihedral angles are the default values in the Build Protein module of Discovery Studio 3.1 (Accelrys Inc.). The residues are rendered as sticks with the Asp carbon chains in violet and the Glu carbons in green. B, aspartate. The Asp residue is shown with a C-α to C (O2) distance of 2.642 A. C, glutamate. The Glu residue is shown with a C-α to C (O2) distance of 3.862 A.

provide insight into the structures and mechanisms of glycine and ethanol action.

Substituting charged residues at position 52 in α1GlyRs did not consistently affect the sensitivity of the receptor to glycine. Substituting negatively charged glutamate (A52E) strongly increased the sensitivity of the receptor to glycine as evidenced by a left shift in the glycine concentration response curve. In contrast, substituting the negatively charged A52D significantly right-shifted the sensitivity of GlyR to glycine. We propose that this effect might reflect the subtle difference in the side-chain structures of these two amino acids. That is, the additional carbon in the side-chain of glutamate increases the extended length of this amino acid side chain by 1 Å. We conjectured that this extended length could place the charge in a position that is more likely to interact with surrounding positively charged elements such as Arg218 in the pre-M1 region (Castaldo et al., 2004) or Lys276 in neighboring subunits. The latter positively charged residues have been shown to be in positions favorable to form salt bridges with Glu53 in loop 2 and Asp138 in loop 7 (Kash et al., 2004; Crawford et al., 2008; Perkins et al., 2009; Nury et al., 2010).

The conclusion that the presence of a negative charge is not the only factor in determining the sensitivity of α1GlyRs to agonist is further supported by our study in which we bound the negatively charged MTSES reagent to position 52. This addition did not alter agonist sensitivity. Prior studies indicate that this lack of effect cannot be attributed to the inaccessibility of MTSES to position 52 (Crawford et al., 2007, 2008; Cederholm et al., 2010). Moreover, binding a neutral MTS reagent to a cysteine substitution at position 53 did not alter the sensitivity of the mutant receptor to agonist (Crawford et al., 2008). This evidence, taken in context with the proximity of position 52 to 53 and the specific geometry of loop 2, suggests that the lack of effect of MTSES at position 52 cannot be attributed to the added volume of the MTS reagent. From these findings, we conclude that the mere presence of a negative charge at position 52 is not sufficient for determining agonist sensitivity.

It is noteworthy that substituting glutamine, the uncharged structural analog of glutamate, at position 52 (A52Q) did not significantly affect glycine sensitivity. Whereas substituting asparagine, the uncharged structural analog of negatively charged aspartate, at position 52 (A52N) drastically decreased agonist sensitivity and markedly reduced I_{max}. Biotinylation followed by Western blot indicated that this change in I_{max} cannot be explained by a reduction in cell surface expression. Therefore, it is possible that the substitution of asparagine at position 52 allows formation of a salt bridge across the β hairpin of loop 2 (Fig. 6E) that results in a change in the conformation and dynamics of loop 2.

Collectively, these findings probing the role of charge and structure at position 52 indicate that charge per se is not the only factor controlling glycine sensitivity. Rather, the presence of a negative charge, combined with a specific geometry of the amino acids, can have a major effect on the sensitivity of α1GlyRs to agonist.

The overall effects of substituting charged residues at position 52 on the sensitivity of α1GlyRs to ethanol were similar to the effects of these substitutions on glycine sensitivity. However, there were important differences. As with the glycine EC_{50}, substituting positively charged residues at position 52 did not significantly affect the sensitivity of the receptor to ethanol. In addition, as with glycine EC_{50}, substituting the negatively charged glutamate, but not the negatively charged aspartate, significantly increased the sensitivity of the receptor to ethanol. In contrast to the results for glycine, substituting glutamine, the uncharged structural analog of negatively charged glutamate, also significantly increased ethanol sensitivity. Substituting asparagine, the uncharged structural analog of the negatively charged aspartate, drastically reduced ethanol sensitivity. These findings clearly indicate that it is the structure of glutamate and glutamine, and not the negative charge of glutamate alone, that increased ethanol sensitivity. This conclusion is supported by our demonstration that binding the negatively charged MTSES reagent to A52C did not restore the reduced ethanol sensitivity of the A52C mutant GlyR back to that of WT receptors. As discussed above with respect to glycine, the lack of effect of MTSES cannot be attributed to a lack of accessibility to position 52 (Crawford et al., 2007, 2008; Cederholm et al., 2010).

Therefore, these findings with charged residues do not fit predictions based on the high correlation between the polarity of the residue at position 52 and ethanol sensitivity (Perkins et al., 2008). That is, the structure of the substitution, as well as its charge, is what determined ethanol sensitivity in the present study. In contrast to the interrelationship between charge and the structure of the amino acid substituted at position 52 on glycine sensitivity, the effect of these substitutions on ethanol sensitivity seem to reflect subtle differences only in the structure of the amino acid. Hence, the physical-chemical parameters at position 52 that control sensitivity to glycine are different from those that control sensitivity to ethanol.

The current findings add to prior studies, which have shown that the sensitivity of Ala52 mutant GlyRs to ethanol is not correlated with the glycine EC_{50} (Perkins et al., 2008). Thus, it is unlikely that the changes in ethanol sensitivity produced by these substitutions in the present study result from changes in receptor sensitivity to agonist. Rather, the

evidence indicates that mutations at position 52 can independently affect agonist sensitivity and ethanol sensitivity.

Based on the experimental results, we conclude that these interactions are electrostatic (Xiu et al., 2005), but also include specific interdomain salt bridges as proposed by Kash et al. (2003). The exceptional sensitivity of both alcohol potentiation and glycine EC_{50} to relatively conserved mutations suggests that the exact shape and dynamics of loop 2 are important for both transmission of agonist binding energy and its potentiation by ethanol. Thus, these findings provide a possible structural-functional basis for the important role that loop 2 can play in markedly altering the sensitivity of GlyRs and $GABA_A$Rs to ethanol (Perkins et al., 2009).

In support of this conclusion, the simulations of the loop 2 mutations shown in Fig. 6 describe likely salt bridges that form and interact across the β hairpin of loop 2. These salt bridges are not present in the WT receptor. These electrostatic interactions have the effect of distorting loop 2 and making it more rigid (Fig. 6, C–E). Other electrostatic interactions of loop 2 with parts of the TM domain are thought to be important in the transmission of the energy of ligand binding to the gate of the ion pore (Kash et al., 2003; Xiu et al., 2005). It is possible that the distortions in loop 2 induced by the A52E and A52N mutations alter glycine and ethanol responses by changing the transmission of gating energy, often described as a "conformational wave" (Grosman et al., 2000; Purohit and Auerbach, 2011).

An important result of the present studies is the apparent precision of the salt-bridge interactions in loop 2 that were probed here. Early descriptions of electrostatic interactions between the ligand-binding domain and transmembrane domain showed multiple shared interactions between residues in the TM2–3 linker, loop 2, and loop 7 (Cys-loop) (Kash et al., 2003). We found large differences between A52E and A52D as well as between A52N and A52Q. In each of these examples, the difference in the total length (C-α to C-α) of the corresponding salt bridges is approximately 1Å. That is, these results are best fit by a complex and dynamic pattern of interactions that include favorable electrostatic and geometric interactions versus unfavorable van der Waals interactions.

The short molecular dynamics simulations reported here and by Cheng et al. (2007) are consistent with changes in the electrostatic interactions of loop 2 with the TM2–3 linker (Lys276) described previously (Kash et al., 2003). However, even relatively long time-scale molecular dynamics simulations (1-μs simulation of ethanol binding to GlyR with a large Linux cluster and 6 weeks × 120 of computer time) (Murail et al., 2011) of GlyR in the presence or absence of ethanol do not show substantial changes in the tertiary structure of GlyR.

In summary, the ability of substitutions at position 52 to alter the sensitivity of α1GlyRs to agonist and ethanol reinforces the evidence that position 52 is a site involved in a conformational wave that plays a key role in agonist activation and ethanol modulation. This knowledge will help to define the chemical architecture of this site of ethanol action and the key physical-chemical parameters that cause and antagonize the actions of ethanol in GlyRs.

Acknowledgments

We thank Miriam Fine, Rachel Kelly, Jeffrey Tom, and Drs. Edward Bertaccini and Kaixun Li for technical assistance and scientific input.

Authorship Contributions

Participated in research design: Perkins, Trudell, Davies, and Alkana.

Conducted experiments: Perkins, Trudell, and Asatryan.

Performed data analysis: Perkins, Davies, and Alkana.

Wrote or contributed to the writing of the manuscript: Perkins, Trudell, Asatryan, Davies, and Alkana.

References

Baenziger JE and Corringer PJ (2011) 3D structure and allosteric modulation of the transmembrane domain of pentameric ligand-gated ion channels. *Neuropharmacology* **60:**116–125.

Bertaccini EJ, Wallner B, Trudell JR, and Lindahl E (2010) Modeling anesthetic binding sites within the glycine α one receptor based on prokaryotic ion channel templates: the problem with TM4. *J Chem Inf Model* **50:**2248–2255.

Bocquet N, Nury H, Baaden M, Le Poupon C, Changeux JP, Delarue M, and Corringer PJ (2009) X-ray structure of a pentameric ligand-gated ion channel in an apparently open conformation. *Nature* **457:**111–114.

Castaldo P, Stefanoni P, Miceli F, Coppola G, Del Giudice EM, Bellini G, Pascotto A, Trudell JR, Harrison NL, Annunziato L, et al. (2004) A novel hyperekplexia-causing mutation in the pre-transmembrane segment 1 of the human glycine receptor α1 subunit reduces membrane expression and impairs gating by agonists. *J Biol Chem* **279:**25598–25604.

Cederholm JM, Absalom NL, Sugiharto S, Griffith R, Schofield PR, and Lewis TM (2010) Conformational changes in extracellular loop 2 associated with signal transduction in the glycine receptor. *J Neurochem* **115:**1245–1255.

Chen ZW, Chang CS, Leil TA, Olcese R, and Olsen RW (2005) GABAA receptor-associated protein regulates GABAA receptor cell-surface number in *Xenopus laevis* oocytes. *Mol Pharmacol* **68:**152–159.

Cheng MH, Cascio M, and Coalson RD (2007) Homology modeling and molecular dynamics simulations of the α1 glycine receptor reveals different states of the channel. *Proteins* **68:**581–593.

Crawford DK, Perkins DI, Trudell JR, Bertaccini EJ, Davies DL, and Alkana RL (2008) Roles for loop 2 residues of α1 glycine receptors in agonist activation. *J Biol Chem* **283:**27698–27706.

Crawford DK, Trudell JR, Bertaccini EJ, Li K, Davies DL, and Alkana RL (2007) Evidence that ethanol acts on a target in loop 2 of the extracellular domain of α1 glycine receptors. *J Neurochem* **102:**2097–2109.

Davies DL, Crawford DK, Trudell JR, Mihic SJ, and Alkana RL (2004) Multiple sites of ethanol action in α1 and α2 glycine receptors suggested by sensitivity to pressure antagonism. *J Neurochem* **89:**1175–1185.

Davies DL, Trudell JR, Mihic SJ, Crawford DK, and Alkana RL (2003) Ethanol potentiation of glycine receptors expressed in Xenopus oocytes antagonized by increased atmospheric pressure. *Alcohol Clin Exp Res* **27:**743–755.

Grosman C, Zhou M, and Auerbach A (2000) Mapping the conformational wave of acetylcholine receptor channel gating. *Nature* **403:**773–776.

Hibbs RE and Gouaux E (2011) Principles of activation and permeation in an anion-selective Cys-loop receptor. *Nature* **474:**54–60.

Karlin A and Akabas MH (1998) Substituted-cysteine accessibility method. *Methods Enzymol* **293:**123–145.

Kash TL, Jenkins A, Kelley JC, Trudell JR, and Harrison NL (2003) Coupling of agonist binding to channel gating in the $GABA_A$ receptor. *Nature* **421:**272–275.

Kash TL, Kim T, Trudell JR, and Harrison NL (2004) Evaluation of a proposed mechanism of ligand-gated ion channel activation in the GABAA and glycine receptors. *Neurosci Lett* **371:**230–234.

Lynch JW (2004) Molecular structure and function of the glycine receptor chloride channel. *Physiol Rev* **84:**1051–1095.

Mascia MP, Machu TK, and Harris RA (1996a) Enhancement of homomeric glycine receptor function by long-chain alcohols and anaesthetics. *Br J Pharmacol* **119:**1331–1336.

Mascia MP, Mihic SJ, Valenzuela CF, Schofield PR, and Harris RA (1996b) A single amino acid determines differences in ethanol actions on strychnine-sensitive glycine receptors. *Mol Pharmacol* **50:**402–406.

Meera P, Olsen RW, Otis TS, and Wallner M (2010) Alcohol- and alcohol antagonist-sensitive human GABAA receptors: tracking δ subunit incorporation into functional receptors. *Mol Pharmacol* **78:**918–924.

Mihic SJ, Ye Q, Wick MJ, Koltchine VV, Krasowski MD, Finn SE, Mascia MP, Valenzuela CF, Hanson KK, Greenblatt EP, et al. (1997) Sites of alcohol and volatile anaesthetic action on $GABA_A$ and glycine receptors. *Nature* **389:**385–389.

Mody I, Glykys J, and Wei W (2007) A new meaning for "Gin & Tonic": tonic inhibition as the target for ethanol action in the brain. *Alcohol* **41:**145–153.

Molander A, Lidö HH, Löf E, Ericson M, and Söderpalm B (2007) The glycine reuptake inhibitor Org 25935 decreases ethanol intake and preference in male wistar rats. *Alcohol Alcohol* **42:**11–18.

Molander A and Söderpalm B (2005) Accumbal strychnine-sensitive glycine receptors: an access point for ethanol to the brain reward system. *Alcohol Clin Exp Res* **29:**27–37.

Murail S, Wallner B, Trudell JR, Bertaccini E, and Lindahl E (2011) Microsecond simulations indicate that ethanol binds between subunits and could stabilize an open-state model of a glycine receptor. *Biophys J* **100:**1642–1650.

Nury H, Poitevin F, Van Renterghem C, Changeux JP, Corringer PJ, Delarue M, and Baaden M (2010) One-microsecond molecular dynamics simulation of channel gating in a nicotinic receptor homologue. *Proc Natl Acad Sci U S A* **107:**6275–6280.

Nury H, Van Renterghem C, Weng Y, Tran A, Baaden M, Dufresne V, Changeux JP, Sonner JM, Delarue M, and Corringer PJ (2011) X-ray structures of general anaesthetics bound to a pentameric ligand-gated ion channel. *Nature* **469:**428–431.

Olsen RW, Hanchar HJ, Meera P, and Wallner M (2007) GABAA receptor subtypes: the "one glass of wine" receptors. *Alcohol* **41:**201–209.

Perkins DI, Trudell JR, Crawford DK, Alkana RL, and Davies DL (2008) Targets for ethanol action and antagonism in loop 2 of the extracellular domain of glycine receptors. *J Neurochem* **106:**1337–1349.

Perkins DI, Trudell JR, Crawford DK, Alkana RL, and Davies DL (2010) Molecular targets and mechanisms for ethanol action in glycine receptors. *Pharmacol Ther* **127:**53–65.

Perkins DI, Trudell JR, Crawford DK, Asatryan L, Alkana RL, and Davies DL (2009) Loop 2 structure in glycine and $GABA_A$ receptors plays a key role in determining ethanol sensitivity. *J Biol Chem* **284:**27304–27314.

Pless SA and Lynch JW (2009) Magnitude of a conformational change in the glycine receptor β1-β2 loop is correlated with agonist efficacy. *J Biol Chem* **284:**27370–27376.

Ponder JW and Richards FM (1987) Tertiary templates for proteins. Use of packing criteria in the enumeration of allowed sequences for different structural classes. *J Mol Biol* **193:**775–791.

Purohit P and Auerbach A (2011) Glycine hinges with opposing actions at the acetylcholine receptor-channel transmitter binding site. *Mol Pharmacol* **79:**351–359.

Rajendra S, Lynch JW, and Schofield PR (1997) The glycine receptor. *Pharmacol Ther* **73:**121–146.

Santhakumar V, Wallner M, and Otis TS (2007) Ethanol acts directly on extrasynaptic subtypes of GABAA receptors to increase tonic inhibition. *Alcohol* **41:**211–221.

Wallner M, Hanchar HJ, and Olsen RW (2003) Ethanol enhances α4β3δ and α6β3δ γ-aminobutyric acid type A receptors at low concentrations known to affect humans. *Proc Natl Acad Sci U S A* **100:**15218–15223.

Webb TI and Lynch JW (2007) Molecular pharmacology of the glycine receptor chloride channel. *Curr Pharm Des* **13:**2350–2367.

Xiu X, Hanek AP, Wang J, Lester HA, and Dougherty DA (2005) A unified view of the role of electrostatic interactions in modulating the gating of Cys loop receptors. *J Biol Chem* **280:**41655–41666.

Zhu F and Hummer G (2010) Pore opening and closing of a pentameric ligand-gated ion channel. *Proc Natl Acad Sci U S A* **107:**19814–19819.

Address correspondence to. Daryl L. Davies, University of Southern California School of Pharmacy, 1985 Zonal Avenue, PSC 500, Los Angeles, CA 90089. E-mail: ddavies@usc.edu